A Sequential Quadratic Programming Approach for the Predictive Control of the COVID-19 Spread ⋆

Marcelo M. Morato [*,**] **Gulherme N. G. dos Reis** [*]
Julio E. Normey-Rico [*]

[*] *Dept. de Automação e Sistemas (*DAS*), Univ. Fed. de Santa Catarina, Florianópolis-SC, Brazil. (marcelomnzm@gmail.com)*
[**] *Univ. Grenoble Alpes, CNRS, Grenoble INP*$^{\top}$*, GIPSA-lab, 38000 Grenoble, France.* $\top$*Institute of Engineering Univ. Grenoble Alpes.*

Abstract: The COVID-19 pandemic is the defying crisis of our time. Since mass vaccination has not yet been established, countries still have been facing many issues due to the viral spread. Even in cities with high seroprevalence, intense resurgent waves of COVID-19 have been registered, possibly due to viral variants with greater transmission rates. Accordingly, we develop a new Model Predictive Control (MPC) framework that is able to determine social distancing guidelines and altogether provide estimates for the future epidemiological characteristic of the contagion. For such, the viral dynamics are represented through a Linear Parameter Varying (LPV) version of the Susceptible-Infected-Recovered-Deceased (SIRD) model. The solution of the LPV MPC problem is based on a Sequential Quadratic Program (SQP). This SQP provides convergent estimates of the future LPV scheduling parameters. We use real data to illustrate the efficiency of the proposed method to mitigate this contagion while vaccination is ongoing.

Keywords: Model Predictive Control, Linear Parameter Varying Systems, COVID-19.

1. INTRODUCTION

The SARS-CoV-2 virus causes a severe acute respiratory syndrome, which can become potentially fatal. This virus has spread rapidly and efficiently, becoming a worldwide pandemic since the beginning of 2020. As of April, 2021, 130 million COVID-19 cases have been confirmed worldwide, with over 2.8 million deaths. Vaccines for this virus have been developed and are currently being applied worldwide (Le et al., 2020). Nevertheless, the vaccination landscape is somewhat slow and, in many countries, still reduced to focus groups. Complementary, many concerning variants of this virus are being registered in all continents (Mallapaty, 2021). We highlight the case of Manaus, Brazil (Sabino et al., 2021), where an intense resurgence of COVID-19 was registered in the beginning of 2021, despite the high seroprevalence verified in the region. The effects of the local viral variant with greater transmission rate corroborate with the thesis that a "natural" herd immunity threshold is unreachable (Taylor, 2021).

Therefore, the public health tactic of social distancing is still the most pertinent alternative to control and end the COVID-19 while vaccination does not reach a high percentage of the susceptible population, as argue Fontanet et al. (2021). The concept of social distancing is, as of today, very well established and understood: in order to prevent the saturation of health systems due to large amounts of COVID-19 hospitalisations at the same time, social distancing measures are able to dilute the demand for treatment over time.

Many recent results indicate that Model Predictive Control (MPC) schemes provide an efficient framework to plan adequate social distancing measures, theoretically able to mitigate infection levels, thus maintain Intense Care Unit (ICU) occupancy rates below boundary-critical thresholds. These algorithms have been formulated using robust tools (Köhler et al., 2020), on-off design (Morato et al., 2020a), parametric formulations (Morato et al., 2020b), and so forth (Pataro et al., 2021). The great majority of works consider static contagion models (SIRD, SIDARTHE, and other variations). Nevertheless, the most recent literature points out to the fact that the COVID-19 disease exhibits inherent time-varying epidemiological characteristics (transmission rate, lethality, etc), e.g. Calafiore et al. (2020). This issue has become specially evident with the rise of the new viral variants (Fontanet et al., 2021).

In light of the previous discussion, the main contribution of this paper is a novel optimisation-based solution for the predictive control of the COVID-19 pandemic, taking into account time-varying contagion characteristics. The proposed method generates weekly social distancing guidelines altogether with accurate estimates for the future behaviour of the pandemic. The time-varying characteristics of the contagion are represented with a Linear Parameter Varying (LPV) Susceptible-Infected-Recovered-Deceased (SIRD) model (Sec. 2). Then, the LPV MPC problem is solved through a Sequential Quadratic Program (SQP) (Sec. 3). As a complementary contribution, we demon-

⋆ This work has been supported by *CNPq* (304032/2019 − 0). We thank Prof. E. Camponogara for his valuable comments and suggestions on the original draft.

strate that this SQP solution ensures convergent estimates of the future LPV scheduling parameters (Sec. 4). Using the data of Florianópolis, Brazil as benchmark, we provide simulation results of the proposed control method (Sec. 5).

2. LPV SIRD MODEL

Recent literature has demonstrated how the SARS-CoV-2 viral contagion dynamics can be appropriately described by SIRD models (González et al., 2020). These models describe the viral spread w.r.t. a population that is split into four non-intersecting classes: (1) the total amount of susceptible individuals $S(k)$, which are prone to contract the disease; (2) the individuals that are currently infected with the disease $I(k)$; (3) the total amount of recovered individuals $R(k)$; and (4) the total amount of deceased individuals $D(k)$. Through the sequel, we denote these four variables as the state variables $x(k)$, which are measurable. Note that the total population size $N(k)$ is given as the sum of the first three classes.

Through the sequel, we consider weekly samples k, with $T_s = 7$ days. This is done in order to account for the average incubation period of the virus, and so that social distancing guidelines do no change so often (refer to the discussion in (Morato et al., 2020a)).

There are three epidemiological parameters in SIRD models: (1) the transmission rate parameter β, which represents the average number of contacts that are sufficient for transmission of the virus from one individual to another; (2) the infectiousness Poisson parameter γ, which stands for the inverse of the period of time for which a given infected individual is indeed infectious; and (3) the mortality rate parameter ρ, which gives the ratio of infected individuals that die. Following the lines of previous works, e.g. (Morato et al., 2020b; Calafiore et al., 2020; Fontanet et al., 2021), we incorporate the time-varying characteristics of these parameters by considering them as state-dependent maps. Accordingly, the time-varying SIRD model is as follows:

$$
\begin{aligned}
S(k+1) &= \left(1 - \overbrace{T_s \frac{\beta(k) I(k)}{N(k)}}^{a_S(k)}\right) S(k) + a_S(k) S(k) u(k)\,, \\
I(k+1) &= \left(1 + T_s \frac{\beta(k) S(k)}{N(k)} - T_s \frac{\gamma(k)}{1-\rho(k)}\right) I(k) \\
&\quad - \left(T_s \frac{\beta(k) I(k) S(k)}{N(k)}\right) u(k)\,, \\
R(k+1) &= R(k) + \left(T_s \gamma(k)\right) I(k)\,, \\
D(k+1) &= D(k) + \left(T_s \frac{\rho(k)}{1-\rho(k)}\right) I(k)\,,
\end{aligned}
$$

considering the following time-varying epidemiological characteristics, with $I_{\max}$ and $D_{\max}$ being the worst-case infections and lethality expectations, respectively:

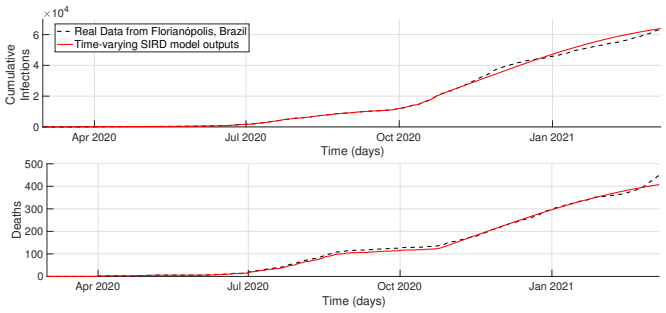

Fig. 1. Time-Varying SIRD Model Validation: Data from Florianópolis, Brazil.

$$
\begin{aligned}
\beta(k) = f_\beta(I(k)) &= \beta_0 + \frac{I(k)}{I_{\max}} \beta_1\,, \\
\gamma(k) = f_\gamma(I(k)) &= \gamma_0 - \frac{I(k)}{I_{\max}} \gamma_1\,, \\
\rho(k) = f_\rho(D(k)) &= \rho_0 + \frac{D(k)}{D_{\max}} \rho_1\,.
\end{aligned}
$$

We note that the state-dependent maps $f_\beta(I(k))$, $f_\gamma(I(k))$ and $f_\rho(D(k))$ are coherent with epidemiological discussions: the virus is more transmissible and more infectious at moments of great infection peaks, and more lethal at moments of elevated fatalities (as empirically observed in Manaus (Sabino et al., 2021)). We consider the active symptomatic infections as $p_{\text{sym}} I(k+i)$. Parameters β_0, γ_0 and ρ_0 stand for nominal transmission, infection and lethality rates, respectively, while β_1, γ_1 and ρ_1 can be understood as supplementary rates, which intensify the contagion spread whenever $I(t)$ gets close to $I_{\max}$.

In this model, the control input $u \in [0, 1]$ represents the social distancing level: $u = 1$ represents a total lockdown situation, with no social interactions, whereas $u = 0$ stands for the complete opposite: all the susceptible population in constant interaction. In practice, we use $\mathcal{U} := \{u \in \mathbb{R} \,|\, 0.3 \leq u \leq 0.7\}$, which represents the set of feasible social distancing values (Morato et al., 2020a).

In order to illustrate the effectiveness of this time-varying SIRD model with the proposed state-dependent epidemiological maps to capture the contagion spread phenomenon, Fig. 1 compares model-based predictions with real data from Florianópolis, Brazil. The model mismatch is considerably small.

As thoroughly exploited and debated by González et al. (2020), SIR-type posses only local $\epsilon - \delta$ stability proprieties. Furthermore, the time-varying SIRD model presented in the prequel is highly nonlinear and possibly nonconvex for specific combinations of the time-varying parameters. Therefore, in order to avoid such inconveniences, we exploit an exact LPV embedding of the viral dynamics. LPV models offer reduced conservativeness, being linear on the state space and thus convex for fixed parameter values. Since we seek a MPC algorithm application in order to generate social distancing guidelines, the LPV framework becomes a welcome solution, leading to convex programs. We further elaborate on this topic in Sec. 3.

Exploiting the fact that the states $x(k)$ are measurable, consider the following exact LPV realisation:

$$x(k+1) = A(\theta(k))x(k) + B(\theta(k))u(k)\,, \tag{1}$$
$$\theta(k) = f_\theta(x(k))\,, \tag{2}$$

where $\theta := \left[\left(\frac{f_\beta(I)I}{N}\right)\ f_\beta(I)\ \frac{f_\gamma(I)}{1-f_\rho(D)}\ f_\gamma(I)\ \frac{f_\rho(D)}{1-f_\rho(D)} \right]^T$ represents scheduling variables, which vary according to the epidemiological characteristics. The scheduling proxy $f_\theta(k)$ is measurable at each sampling instant k and bounded to a known convex set Ω.

In practice, since we deploy a prediction control scheme, we are concerned with the state trajectory behaviour along the future N_p steps. This prediction horizon slides forward, at each sampling instant k. Thereof, we extend Eq. (1) in order to get the following N_p-horizon trajectories:

$$\mathbf{x} = \mathcal{A}(\Theta)x(k) + \mathcal{B}(\Theta)\mathbf{u}\,, \tag{3}$$

where $\mathbf{x} := \text{col}(x(k) \dots x(k+N_p|k))$ represents the predicted state trajectory sequence, $\Theta := \text{col}(\theta(k) \dots \theta(k+N_p-1))$ gives the real scheduling trajectory, and $\mathbf{u} := \text{col}(u(k|k) \dots u(k+N_p-1|k))$ stands for the sequence of control inputs. $\mathcal{A}(\Theta)$ and $\mathcal{B}(\Theta)$ are given below [1].

$$\mathcal{A}(\Theta) = \begin{bmatrix} A(\theta(k)) \\ A(\theta(k+1))A(\theta(k)) \\ \vdots \\ \left(\Pi_{i=0}^{N_p-1} A(\theta(k+i))\right) \end{bmatrix}, \quad \mathcal{B}(\Theta) =$$

$$\begin{bmatrix} B(\theta(k)) & \dots & \left(\Pi_{i=1}^{N_p-1} A(\theta(k+i))\right) B(\theta(k)) \\ 0 & \ddots & \left(\Pi_{i=2}^{N_p-1} A(\theta(k+i))\right) B(\theta(k+1)) \\ \vdots & \dots & \vdots \end{bmatrix}^T .$$

3. THE LPV MPC SCHEME

3.1 The Predictive Control Formulation

As previously discussed, our aim in this paper is to find an optimal control sequence $\mathbf{u}$ for Eq. (3) taking into account the following objectives: (i) minimisation of the number of active infections $I(k)$, (ii) reduction (as much as possible) of the social distancing measures, and (iii) upper-bounding of the active symptomatic infections, which should not surpass the number of available ICU beds in local hospitals (threshold given by n_{ICU}).

In order to encompass these goals, we consider the following quadratic cost function:

$$J_k = \sum_{i=1}^{N_p} \|I(k+i|k)\|_q^2 + \|u(k+i|k)\|_r^2 \tag{4}$$
$$= \mathbf{x}^T \underbrace{(q\mathbb{I}_{n_x})}_{Q} \mathbf{x} + \mathbf{u}^T \underbrace{(r\mathbb{I}_{n_u})}_{R} \mathbf{u}\,,$$

where $q = \frac{(1-r)}{I_{\max}^2}$ and $r \in [0,1]$ are scalar weights used to tune the trade-off between objectives (i) and (ii).

Objective (iii) is implied through the following constraint:

$$p_{\text{sym}} I(k+i) \leq n_{\text{ICU}}, \forall i \in \mathbb{N}_{[1,N_p]}\,. \tag{5}$$

Thus, the proposed social distancing strategy for the COVID-19 contagion spread is based on the following MPC optimisation problem:

$$\begin{aligned} \mathbf{u} &= \min_{\mathbf{u}} J_k \\ \text{s.t.} \quad & \mathbf{x} = \mathbf{A}(\Theta)x(k) + \mathcal{B}(\Theta)\mathbf{u}\,, \\ & A_x\mathbf{x} \leq b_x\,,\ \ A_u\mathbf{u} \leq b_u\,. \end{aligned} \tag{6}$$

Note that, in Problem (6), the inequality constraints are used to ensure objective (iii) and that each control signal is given within the social distancing feasibility set $\mathcal{U}$. A_x, A_u, b_x and b_u are obtained by manipulating the constraints. Furthermore, J_k admits constant weights q and r, chosen to tune the obtained response.

The state trajectories $\mathbf{x}$ can be computed using $\Theta = f_\theta(\mathbf{x})$, as gives Eq. (2). Nevertheless, using such "full-blown" nonlinear description of the SIRD trajectories would convert the optimisation problem (6) into a Nonlinear Program (NP), which has increased computational complexity. Furthermore, the solution of an NP may have local minima, which is undesirable.

Recent literature (e.g. (González Cisneros and Werner, 2020)) has shown how that NPs can be converted into QPs with an adequate replacement of nonlinear scheduling proxy $\Theta = f_\theta(\mathbf{x})$ by iterative estimates $\Theta(l)$. By doing so, numerical burden is relieved and a global minima J_k of can be founf w.r.t. $\Theta(l)$. This approach is attractive because the nonlinear state predictions and constraints are handled linearly at each iteration, which is rather cost-efficient. In the sequel, we describe the method with more details.

3.2 Method Decription

The core idea of the SQP method is as follows: the MPC represented by Problem (6) is solved multiple times based on an iterative frozen prediction model $\mathbf{x} = \mathcal{A}(\Theta(l))x(k) + \mathcal{B}(\Theta(l))\mathbf{u}$, which is scheduled according to $\Theta(l)$ at the l-th iteration. At each iteration, the scheduling trajectory $\Theta(l)$ is taken as $f_\theta(\mathbf{x}(l-1))$, where $\mathbf{x}(l-1)$ indicates the state predictions made at the $(l-1)$-th iteration of the following optimisation problem:

$$\begin{aligned} \mathbf{u}(l) &= \min_{\mathbf{u}(l)} J_k \\ \text{s.t.} \quad & \mathbf{x}(l) = \mathcal{A}(\Theta(l))x(k) + \mathcal{B}(\Theta)(l)\mathbf{u}(l)\,, \\ & A_x\mathbf{x}(l) \leq b_x\,,\ \ A_u\mathbf{u}(l) \leq b_u\,. \end{aligned} \tag{7}$$

Problem (7) is a QP, since the state predictions are linear (matrices $\mathcal{A}(\Theta(l))$ and $\mathcal{B}(\Theta(l))$ are constant [2]). We stress that evaluating $\Theta(l) = f_\theta(\mathbf{x}(l-1))$ outside of the optimisation procedure is much simpler than evaluating it internally as does Problem (6), since the nonlinearities become static and thus are not spanned over the horizon.

This mechanism has the complexity of an SQP since Problem (7) is solved sequentially, multiple times at each sampling instant k. We note that the iterative operations

[1] $\Pi(\cdot)$ denotes the left-side product operator.

[2] These nonlinear matrices maintain the same form at each iteration l and, thus, can be efficiently computed.

stop when the scheduling sequence estimate $\Theta(l)$ converges to the true scheduling sequence trajectory Θ. We will demonstrate this property (convergence) in Sec. 4.

The major advantage of this SQP framework is that this convergence property is established within a relatively small number of iterations l. Since an SQP is solved at each sampling instant k, the framework also serves for time-critical applications. Another interesting property is that, at each sampling instant k, we get an estimate for the future scheduling trajectory Θ, which, in the COVID-19 context, serves to forecast of the future behaviour of the contagion spread.

The SQP mechanism is implemented as gives Algorithm 1. The application departs from an initial state sequence $\mathbf{x}$ and an initial scheduling sequence Θ. These vectors can be simply taken as N_p repeated instances of $x(0)$ and $\theta(0)$. Note that the internal loop stops when convergence is established or when a stop criterion is reached.

Algorithm 1 LPV MPC

Initialise: $x(0) = x_0$, $\theta(0) = \theta(0)$, $k = 0$.
Require: Q, R, N_p, $\mathbf{x}$, Θ. **Loop**:

- Step (1): **Loop until convergence/stop criterion**:
  (i) Based on $\Theta(l) = f_\theta(\mathbf{x}(l))$, compute Eq. (3);
  (ii) Solve the optimisation in Eq. (7);
- Step (3): Apply $u(k)$ to the process;
- Step (4): $k \leftarrow k + 1$.

end

4. SCHEDULING PARAMETER CONVERGENCE

In this Section, we discuss the convergence property of the SQP implementation of the LPV MPC problem (Algorithm 1). This is, we focus on the convergence of $\Theta(l)$ from the SQP to Θ (the real scheduling trajectory in Eq. (3)). We stress that this property is essential, since only with $\Theta(l^\star) \to \Theta$ we can conclude that the control solution $\mathbf{u}(l^\star)$ will be a minimizer of J_k w.r.t. the real system trajectories in Eq. (3). This conversely means that the $J_k|_{\mathbf{u}(l^\star)}$ is a local minimum of J_k for $\mathbf{x}(l^\star) = \mathcal{A}(\Theta(l^\star)x(k) + \mathcal{B}(\Theta)\mathbf{u}(l^\star)$ but also a global minimum of J_k w.r.t. Eq. (3).

Lemma 1. Convergence of Scheduling Trajectory Assume $\Theta = f_\theta(\mathbf{x})$ is bijective. Consider that matrices $\mathcal{A}(\Theta)$ and $\mathcal{B}(\Theta)$ are well-defined on Θ. Take $\hat{\Theta} := \text{col}\{\theta^0\, \theta^1\, \ldots\, \theta^{N_p-1}\}$. Suppose there exist a symmetric positive definite matrix $Y \in \mathbb{R}^{(N_p n_x)\times(N_p n_x)}$ and a rectangular matrix $W \in \mathbb{R}^{(N_p n_u)\times(N_p n_x)}$. The scheduling trajectory estimate $\hat{\Theta} := \Theta(l)$ converges to the real trajectory Θ within a finite number of iterations l if the following LMI holds for all $\theta^0, \ldots, \theta^{N_p-1} \in \Omega$:

$$\left[\begin{array}{cc|cc} 0 & Y\mathcal{A}^T(\hat{\Theta}) & 0 & Y\mathcal{A}(\hat{\Theta}) \\ \mathcal{A}(\hat{\Theta})Y & -Y & \mathcal{B}(\hat{\Theta})W & -Y \\ \hline \star & \star & 0Y & \\ \star & \star & \star & Y \end{array}\right] < 0\,. \qquad (8)$$

Proof 1. Define the state-feedback $\mathbf{u}(l) := K\mathbf{x}(l)$, with $K = WP$ and $P = Y^{-1} \succ 0$. Apply two consecutive Schur complements to Ineq. (8) and pre-/post-multiply the result by $[x^T(k)\, \mathbf{x}^T(l)]$ in order to get: $\Big(\mathcal{A}(\hat{\Theta})x(k) + \mathcal{B}(\hat{\Theta})K\mathbf{x}(l)\Big)^T P \Big(\mathcal{A}(\hat{\Theta})x(k) + \mathcal{B}(\hat{\Theta})K\mathbf{x}(l)\Big) - \big(\mathbf{x}(l)^T P\mathbf{x}(l)\big) < 0$. Define the storage function $V(l) := \mathbf{x}^T(l)P\mathbf{x}$ in order to get $V(l+1) - V(l) < 0$. It follows that the storage function is decreasing over the iterations l if LMI (8) holds. Since $V(l) > 0$ by definition, the LMI implies in the asymptotic stability of $\mathbf{x}(l)$ at some iteration $l^\star$. Conversely, this means that $\mathbf{x}(l^\star + 1) = \mathbf{x}(l^\star)$ and thus $\Theta(l^\star{+}1) = \Theta(l^\star)$ since $\Theta(l) := f_\theta(\mathbf{x}(l))$. Using the real prediction model from Eq. (3), we obtain $\mathbf{x} := \mathcal{A}(f_\theta(\mathbf{x}))x(k) + \mathcal{B}(f_\theta(\mathbf{x}))K\mathbf{x}$. Since we assume that $f_\theta(\cdot)$ is bijective, there exists only one possible $\Theta := f_\theta(\mathbf{x})$ such that Eq. (3) holds, which means that $\mathbf{x}$ is a global attractor for $\mathbf{x}(l)$. Therefore $\Theta(l^\star) = f_\theta(\mathbf{x}(l^\star)) \to \Theta = f_\theta(\mathbf{x})$. This concludes the proof.

Remark 1. Lemma 1 provides infinite-dimensional inequalities, which must hold $\forall\, \theta^0, \ldots, \theta^{N_p-1} \in \Omega$. In practice, the solution can be found by enforcing the LMI over a sufficiently dense grid of points along the $\Omega \times \cdots \times \Omega$ plane. Then, the solution can be verified over a denser grid. If bounded variation rates for the parameters are known, i.e. $\theta(k+1) = \theta(k) + \delta\theta(k)$ with $\delta\theta \in \delta\Omega$, the complexity can be relieved.

Remark 2. We should only verify if LMI problem in Lemma 1 has a parameter-dependent solution Y once (before the actual operation of Algorithm 1). If this is true, this Algorithm will ensure convergence. Otherwise, we cannot guarantee that convergence will be attained. In this case, another option to demonstrate the convergence is to invoke the well-known result for the convergence of Newton SQPs, which implies that a quadratic sub-problem program of SQP algorithms can be derived by a second-order approximation of the SQP optimisation cost and linearisation of its constraints. This discussion is briefly presented in (González Cisneros and Werner, 2020).

5. SIMULATION RESULTS

Considering the time-varying LPV SIRD model and the proposed SQP MPC solution to guide social distancing, we now present simulations results regarding the COVID-19 contagion spread. For such, we consider data from the city of Florianópolis, Brazil [3]. Model parameters were identified using standard methods. Table 1 gathers these parameters together with the used MPC tuning weights. These weights are chosen to ensure a trade-off between infection minimisation and social distancing relaxations, as indicated in (Morato et al., 2020a). The total number of ICU beds in Florianópolis is of $n_{\text{ICU}} = 239$, for a population of approximately 5.10^5 inhabitants. The following results were obtained using Matlab, yalmip and Gurobi.

Table 1. SIRD Parameters and MPC Weights.

β_0	0.0951	β_1	0.0333	γ_0	0.0855
γ_1	$-4.27.10^{-4}$	ρ_0	0.0039	ρ_1	0.0029
T_s	7 days	p_{sym}	39%	$I_{\max}$	750
$D_{\max}$	650	r	0.3	q	$1.43.10^{-5}$

We present two distinct scenarios: (a) comparing the application of the proposed MPC strategy to what in fact was observed in the city Florianópolis (from March 2020 to January 2021); and (b) the use of the MPC strategy to

[3] This city was chosen as a case study, but the method was also tested for other locations, with no loss of generality.

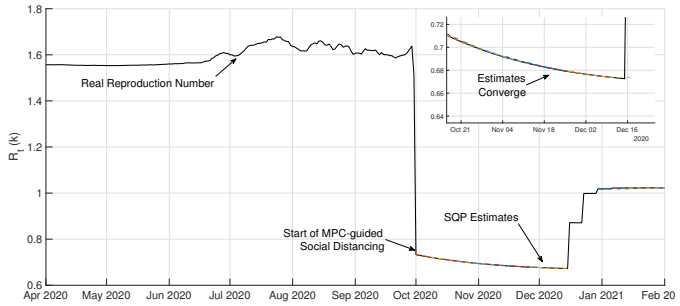

Fig. 2. R_t: Real trajectory and SQP predictions.

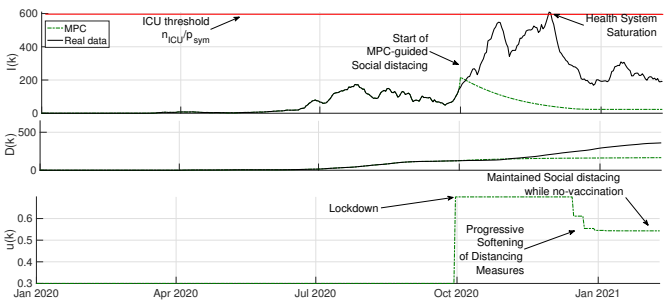

Fig. 3. Scenario (a): MPC vs Data.

guide social distancing from January 2021 onward, taking into account the current vaccination panorama. Recall that the proposed MPC generates weekly social distancing guidelines. The prediction horizon is of $N_p = 4$ weeks.

5.1 Effectiveness of the MPC Approach

In order to demonstrate the effectiveness of the MPC approach to guide social distancing measures in pandemic situations, we consider the COVID-19 data from Florianópolis ranging from December 2020 to April 2021. The actual social distancing level observed in the city in this period was considerably small (close to $u = 0.3$), due to the lack of stronger measures from the federal government and the resistance of the population in really adhering to these measures (Ortega and Orsini, 2020).

Firstly, we note that there exists [4] a positive definite matrix Y, which is a solution of Lemma 1, meaning that the SQP approach indeed converges. In order to illustrate this property, we prefer to show that the future predictions for the effective reproduction number R_t of the contagion, at each weekly sampling instant, are representative.

We note that R_t is an essential epidemiological concept: R_t quantifies the average potential of a given contagion, representing how many cases are expected to be generated due to a single primary case, within a population for which all individuals are susceptible. From a control viewpoint, R_t represents the contagion spread velocity: when $R_t > 1$, the number of infections is increasing, whereas if $R_t \leq 1$, the contagion is ceasing. This time-varying parameter is computed as indicate Morato et al. (2020b):

$$R_t(k) := \frac{\beta(k)(1-\rho(k))}{\gamma(k)} u(k) \;=\; \frac{\theta_2(k)}{\theta_3(k)} u(k)\,,$$

which means that it can be derived from the scheduling trajectory estimates $\Theta(l)$ generated by the SQP framework.

Accordingly, Fig. 2 shows the true model-based effective reproduction number R_t of the contagion and the estimates generated by Algorithm 1 at different sampling instants. As one can see, the estimates are indeed convergent, which means that the generated control solution $\mathbf{u}^\star(l)$ is optimal, since the sequential operation of Eq. (7) becomes equivalent to the original nonlinear program from Eq. (6).

Complementary, Fig. 3 provides the comparison of the real contagion data against what could have been seen if an MPC coordination had been enacted by the beginning of October 2020. This figure shows the total deceased individuals, the number of daily active infections, the ICU threshold $\frac{n_{\mathrm{ICU}}}{p_{\mathrm{sym}}}$, as well as the social distancing guideline.

The MPC orchestrates a stronger social distancing guideline at first, in order to relieve the peak of infections that caused a total occupancy of ICU units in Florianópolis by the end of January, 2021. Evidently, if a coordinated model-based guideline was used, many deaths could have been avoided (over 190). Furthermore, the MPC algorithm is able to plan social distancing measures that are able to continuously maintain the number of acute active infections well below ICU threshold, which is very important. Moreover, the algorithm is able to progressively loosen the strength of the distancing measures, as expected from the trade-off objective J_k. The MPC determines an initial lockdown to harshly attenuate the viral spread, in order to then revert it gradually into an average social distancing guideline while vaccination campaigns do not begin.

5.2 Planning for the Following Months

In order to further assess the qualities of the proposed SQP-based MPC solution for social distancing measures, we consider a scenario with ongoing vaccination. The current vaccination panorama at Florianoópolis is of roughly 2500 vaccinated individuals per day, since the beginning of February. Therefore, we simulate the time-varying SIRD dynamics with an additional removal of the vaccinated individuals from the susceptible population.

Considering this vaccination landscape, we show the expected contagion behaviour for the following months (from January 2021) with MPC-coordinated social distancing measures and without any social distancing (i.e. taking $u(k) = 0.3, \forall k$, as currently observed). Firstly, Fig. 4 shows the decay of the susceptible population S due to vaccination and to infections (with/without MPC coordination), separately. Evidently, the susceptible population tends to a steady-state regime due to infections, while displaying a ramp behaviour w.r.t. the vaccination. This pattern is coherent with the mass-vaccination effectiveness seen elsewhere. The figure also display the MPC coordination results, which generates an intial lockdown that is progressively softened. Note that, in this case, a no-isolation rule could have been set in practice already April, due to the great suppression of infections due to vaccination.

Complementary, Fig. 5 provides the pattern of active infections and deaths in the current vaccination landscape

[4] This matrix is not shown due to lack of space ($Y \in \mathbb{R}^{16\times 16}$).

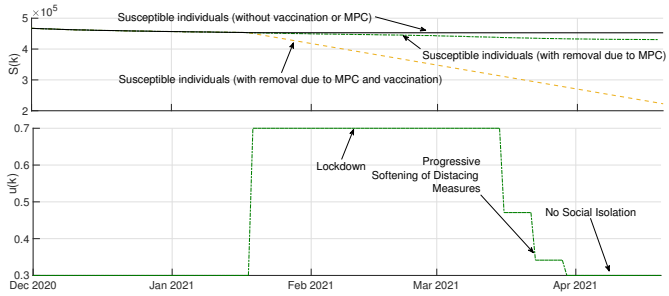

Fig. 4. Scenario (b): Vaccination.

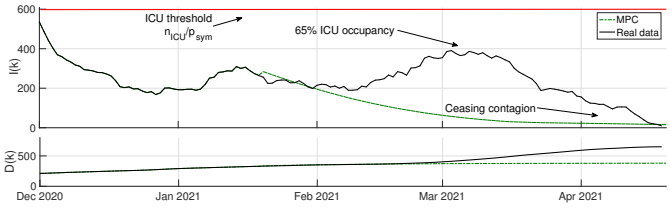

Fig. 5. Scenario (b): Future months with/without MPC.

with and without social distancing measures. These results indicate that if no social distancing is enacted, even with ongoing vaccination, a troublesome scenario would still be seen, since the number of acute infections gets close to the ICU threshold (reaching 65% of occupancy). Moreover, the steady-state regime of a ceased pandemic would only be attained when over 70% of the susceptible population is vaccinated (at the current pace, the forecast indicates this would happen by end-2021). Nevertheless, the results with an MPC-guided social distancing measures indicate that the active infections can get very well controlled, which conversely implies in a "return to pre-COVID-19 life pattern" much earlier, by April 2021, while vaccination reaches the last quarter percentile of the population.

6. CONCLUSIONS

In this paper, we investigated the use of an SQP-based solution for the predictive control of the SARS-CoV-2 viral spread through social distancing measures. In order to develop this procedure, we consider a time-varying SIRD equations represented by an LPV model. The predictive control strategy aims to minimise COVID-19 infections while relaxing social distancing measures as much as possible. Using data from Florianópolis, Brazil, we simulate the effectiveness of the proposed strategy. Our main findings are highlighted: (1) The presented results corroborate the hypothesis that "natural' herd immunity" is not a plausible option. If no coordinated social distancing action is enforced, the ICU threshold gets dangerously tested, which can certainly lead to an elevated number of fatalities; (2) the time-varying viral dynamics can be accurately described with proposed SQP framework, which spans good estimates for the future behaviour of the contagion; (3) the simulation forecasts indicate that social distancing measures should be maintained while mass vaccination is not established. The strength of these measures can be diluted as vaccination progresses.

These results presented in this paper are qualitative. Brazil has not been testing enough its population (neither via mass testing or sampled testing), which means that the data regarding the number of infections is very inconsistent. As discussed by Bastos et al. (2021), the uncertainty margin associated to the available data in the country is very significant. Anyhow, the results presented herein can help long-term regulatory decisions for this pandemic.

REFERENCES

Bastos, S.B., Morato, M.M., Cajueiro, D.O., and Normey-Rico, J.E. (2021). The COVID-19 (SARS-CoV-2) Uncertainty Tripod in Brazil: Assessments on model-based predictions with large under-reporting. *Alexandria Engineering Journal*, 60(5), 4363–4380.

Calafiore, G.C., Novara, C., and Possieri, C. (2020). A time-varying SIRD model for the COVID-19 contagion in Italy. *Annual Reviews in Control*.

Fontanet, A., Autran, B., Lina, B., Kieny, M.P., Karim, S.S.A., and Sridhar, D. (2021). SARS-CoV-2 variants and ending the COVID-19 pandemic. *The Lancet*.

González, A.H., Anderson, A.L., Ferramosca, A., and Hernandez-Vargas, E.A. (2020). Dynamic characterization of control SIR-type systems and optimal single-interval control. URL `https://arxiv.org/abs/2103.11179`. [Pre-print].

González Cisneros, P.S. and Werner, H. (2020). Nonlinear model predictive control for models in quasi-linear parameter varying form. *International Journal of Robust and Nonlinear Control*, 30(10), 3945–3959.

Köhler, J., Schwenkel, L., Koch, A., Berberich, J., Pauli, P., and Allgöwer, F. (2020). Robust and optimal predictive control of the COVID-19 outbreak. *Annual Reviews in Control*.

Le, T.T., Andreadakis, Z., Kumar, A., Román, R.G., Tollefsen, S., Saville, M., Mayhew, S., et al. (2020). The COVID-19 vaccine development landscape. *Nat Rev Drug Discov*, 19(5), 305–306.

Mallapaty, S. (2021). What's the risk of dying from a fast-spreading COVID-19 variant? *Nature*, 590, 191–192.

Morato, M.M., Bastos, S.B., Cajueiro, D.O., and Normey-Rico, J.E. (2020a). An optimal predictive control strategy for COVID-19 (SARS-CoV-2) social distancing policies in brazil. *Annual Reviews in Control*.

Morato, M.M., Pataro, I.M., da Costa, M.V.A., and Normey-Rico, J.E. (2020b). A parametrized nonlinear predictive control strategy for relaxing COVID-19 social distancing measures in Brazil. *ISA transactions*.

Ortega, F. and Orsini, M. (2020). Governing COVID-19 without government in Brazil: Ignorance, neoliberal authoritarianism, and the collapse of public health leadership. *Global public health*, 15(9), 1257–1277.

Pataro, I.M.L., Olivier, J.F., Morato, M.M., Amad, A.A.S., Ramos, P.I.P., Pereira, F.A.C., Silva, M.S., Jorge, D.C.P., Andrade, R.F.S., Barreto, M.L., and da Costa, M.A. (2021). A control framework to optimize public health policies in the course of the COVID-19 pandemic. *Scientific reports*, 11, 13403.

Sabino, E.C., Buss, L.F., Carvalho, M.P., Prete, C.A., Crispim, M.A., Fraiji, N.A., Pereira, R.H., Parag, K.V., da Silva Peixoto, P., Kraemer, M.U., et al. (2021). Resurgence of COVID-19 in Manaus, Brazil, despite high seroprevalence. *The Lancet*, 397(10273), 452–455.

Taylor, L. (2021). COVID-19: Is Manaus the final nail in the coffin for natural herd immunity? *BMJ*, 372.